Supplementary Information for:

Enhanced Frequency Response for Highly Transparent PVDF/Graphene based Thin Film Acoustic Actuator

James S. Lee, Keun-Young Shin, Chanhoi Kim and Jyongsik Jang*

World Class University (WCU) program of Chemical Convergence for Energy & Environment (C_2E_2), School of Chemical and Biological Engineering, College of Engineering, Seoul National University (SNU), Seoul 151-742, Korea.

[*] E-mail: jsjang@plaza.snu.ac.kr
Tel.: +82-2-880-7069
Fax: +82-2-888-1604

Experimental details

Materials: Tetraethyl orthosilicate and titanium (IV) isopropoxide (TTIP, Sigma-Aldrich Chemical Co., USA) and a centrifuge (Mega 17R, Hanil Science and Industrial, South Korea) were used to fabricate the Ba–HNPs. The graphite used in the experiments was purchased from Sigma-Aldrich. Graphene electrodes were printed using a commercial office inkjet printer (Canon Pixima Ip1300). Gases (H_2, CH_4, Ar; 99.99%; Daesung Industrial Gases Co., South Korea), Cu foil (Sigma-Aldrich), and poly(methylmethacrylate) (950 PMMA A4, 4% in anisole, MicroChem Corp., USA) were used in the fabrication of the graphene films. PVDF pellets (molecular weight *ca.* 275,000 by gel permeation chromatography), (3-aminopropyl)trimethoxysilane (APS), and DMF were obtained from Sigma–Aldrich. Commercial PVDF film was obtained from the Fils Corporation (South Korea).

Synthesis of Ba-doped SiO_2/TiO_2 hollow particles (Ba–HNPs): First, 475 mL of ethanol and 17.4 mL of aqueous ammonia were mixed with 17.4 mL of tetraethyl orthosilicate for 12 h at 60°C. Acetonitrile (175 mL) was then added to form a colloidal SiO_2 solution. Second, 21.6 mL of TTIP, 108 mL of ethanol, and 36 mL of acetonitrile were added to the colloidal SiO_2 solution at 5°C, and the mixture was stirred for 12 h. The resulting SiO_2/TiO_2 core/shell nanoparticles precipitated and were isolated by centrifugation. These nanoparticles were resuspended in 500 mL of aqueous $Ba(OH)_2$ solution, which was sonicated for 3 h to disperse the particles. Finally, SiO_2 was etched under basic conditions. The resulting Ba-HNPs were isolated, **approximately 9.6 g**, by centrifugation, redispersed in deionized water, and dried in a vacuum oven at 60°C.

Preparation of the Ba–HNPs/PVDF films: PVDF was dissolved in a 1:1 mixture of DMF, and acetone and Ba–HNPs were added to it. The mixture was sonicated for 2 h to disperse the particles. The solution was transferred into a 12 mL-capacity syringe pump and a 15 kV/cm high voltage was applied between stainless steel plates. The solution was injected onto the collector plate at a constant flow rate of 75 μm/min using the electrospinning process. Ba–HNPs/PVDF nanocomposite fiber was collected on a polyimide film at room temperature and was dried at 60°C in a vacuum oven for 12 h. The dried spun Ba–HNPs/PVDF nanofiber mat on the polyimide film was pressed at 220°C and 800 psi for 1 h and then slowly cooled. The fabricated Ba–HNPs/PVDF films were uniaxially drawn at 10 mm/min to maximize the α-to-β phase transformation; drawing was continued until the film reached 200% of its original length at 90°C while polling was done under a strong constant electric field at 30 kV/mm.

Fabrication of the CVD grown graphene: Cu foil (7 × 7 cm^2) was placed in a glass chamber, and then heated to 1000°C under an 8-sccm flow rate of H_2 gas at 90 mTorr. This condition was maintained for 30 min to condition the inner surface of the glass chamber. Then, a 20 sccm flow of CH_4 gas was drawn into the glass chamber to a total pressure of 560 mTorr, which was held for 40 min. The chamber was then cooled to room temperature at 35°C/min under a H_2 atmosphere. The solution (4%) of PMMA in anisole was spin-coated at 5,000 rpm for 1 min onto the Cu foil. The pristine graphene was isolated after immersing the coated foil into Cu etchant.

Fabrication of the Ba–HNPs/PVDF thin film acoustic actuator: Ba–HNP/PVDF film (7 × 7 cm^2) was treated with a 0.5 wt% aqueous APS solution for 12 h to render the surface hydrophilic. The film was then dried at 60 °C for 6 h. A sandwich structure was fabricated

that consisted of the Ba–HNP/PVDF film sandwiched between CVD grown graphene/PMMA films. The PMMA was removed from the graphene by dissolving in chloroform. **The Cu contact electrode was attached on each corner of fabricated thin film speaker. The sound signal delivered on amplifier and it produced time variable voltage (AC electric field) to produce the sound wave as attractive and repulsive forces. The 9 V battery was used as power supply to operate amplifier and it generated the transformed sound through Ba-HNPs/PVDF thin film.**

***Frequency response and THD testing of fabricated film speaker*: First of all, the fabricated speaker system was installed in soundproofed chamber to avoid reflection interference. The dynamic microphone which is receiving acoustic output signal from film speaker was connected on audio analyzer. The distance between the film speaker and microphone is maintained on 10 cm. The sound source was generated audio signals in each of frequency range, and swept signals were measured by audio analyzer.**

Characterization: High-resolution TEM images were taken using a JEOL JEM-3010 instrument. Field-emission scanning electron microscopy (FE-SEM, JEOL JSM-6700F, Japan) and a FTIR spectrometer (Bomem MB 100, USA) were also used. Atomic force microscopy (AFM, Nanoscope IIIa, Digital instruments, USA) was used to image the surface topography; it was used in the tapping mode with silicon tips at a resonance frequency of 320 kHz. Electrical resistances were measured with a Keithley 2400 source meter at 25°C using the four-probe method. Raman spectra were recorded on a LabRAM HR (Horiba, Japan) with 1064-nm laser excitation. A dScope Series IIIA (Prism Sound Co., UK) audio analyzer was used to determine the acoustic actuator characteristics from 10 Hz to 20 kHz, and these

values were obtained using high quality dynamic microphone (Beyerdynamic, Germany) with maintaining constant distance in soundproof chamber.

1. Characterization of Ba-HNPs.

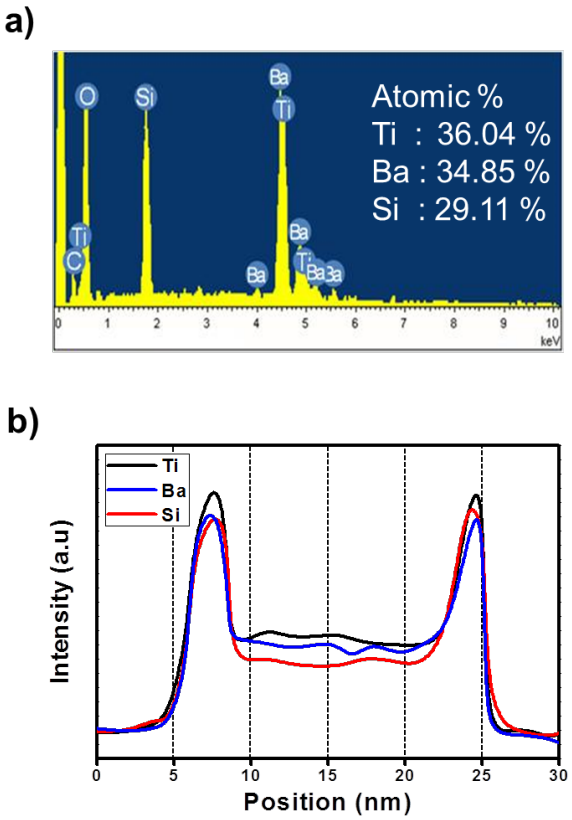

Fig. S1 a) EDX spectra of the Ba-HNPs and EDX analysis of Ba-HNPs elemental contents. Since carbon tape was used to hold Ba-HNPs, atom contents of carbon and oxygen were excluded. b) STEM-EDX line mapping of the Ba-HNPs.

2. Characterization of CVD graphene and photo image of acoustic actuator.

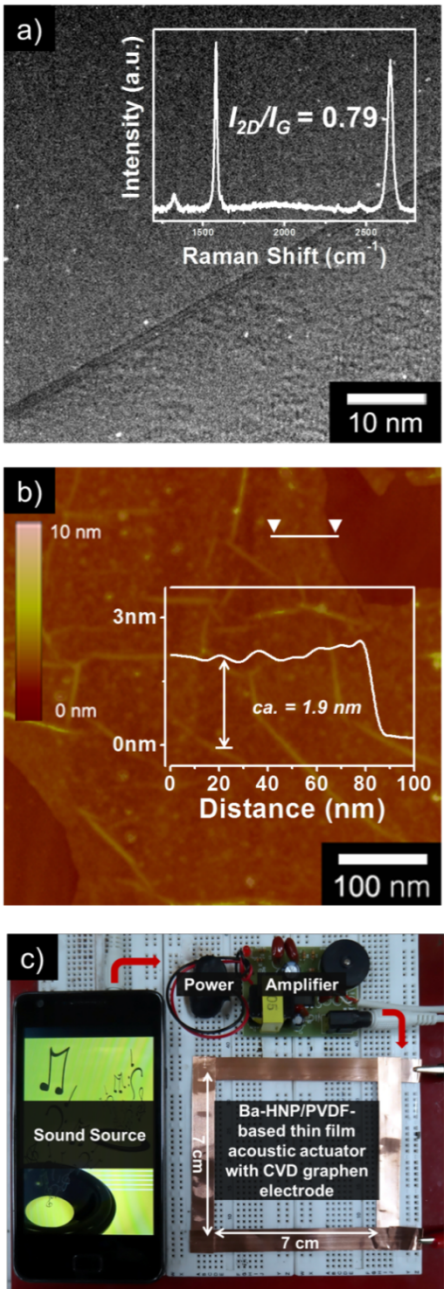

Fig. S2 a) Representation HR-TEM and b) AFM images of CVD grown graphene as an electrode. Inset Raman spectra showed D, G and 2D peaks, and the average thickness of graphene was assumed to be *ca*. 1.9nm. c) Photograph of a Ba-HNPs/PVDF–based thin film acoustic actuator with flexibility and transparency using sandwiched CVD grown graphene electrodes.

The surface of the fabricated thin film was treated with 3-aminopropyltriethoxysilane (APS) coupling agent to improve adhesion to the graphene electrode; reaction occurred between the -OCH_2CH_3 groups of APS with oxygen-containing functional groups such as –OH on the surface of the synthesized CVD graphene. Additionally, the terminal –NH_2 groups of APS reacted with the fluorine atoms of PVDF to form F–H bonds. Hence, the acoustic actuator consisted of a sandwich of a Ba-HNPs/PVDF thin film and CVD graphene electrodes, which was connected to a sound source and amplifier.

3. Mathematical equations for contents of β phase PVDF.

Assuming the IR absorption follows the Lambert-Beer law, content of β phase in PVDF can be measured,

$$F(\beta) = \frac{X_\beta}{X_\alpha + X_\beta} = \frac{A_\beta}{(K_\beta/K_\alpha) + A_\beta} \quad \textbf{(1)}$$

Where A_α and A_β are the absorbance at 766 and 840 cm^{-1} respectively, and K_α (6.1×10^4 cm^2/mol) and K_β (7.7×10^4 cm^2/mol) are the absorption coefficients at the respective wavenumber.

Table S1 β phase content, F(β), for pristine PVDF and various concentration of Ba-HNP/PVDF.

Sample	F(β) (%) [a]
Pristine PVDF	79
10 wt% Ba-HNP/PVDF	87
15 wt% Ba-HNP/PVDF	95
20 wt% Ba-HNP/PVDF	89

a These values were calculated by Lambert-Beer law.

4. Crystallization behavior by filler concentration.

I. Value for obtained crystallinity temperature of fabricated thin film.

Table. S2 Value of T_c for pristine PVDF and various concentrations of Ba-HNPs/PVDF.

Sample	$T^{\alpha}c$ (°C)	$T^{\beta}c$ (°C)
Pristine PVDF	165.76	170.15
10 wt% Ba-HNP/PVDF	-	170.13
15 wt% Ba-HNP/PVDF	-	170.91
20 wt% Ba-HNP/PVDF	-	170.16

II. Mathematical equations for relative degree of DSC.

The relative degree of crystallinity as a function of time, *X(t)*, can be calculated from relative crystallinity as a function of temperature, *X(T)*, by transforming the temperature to a time scale. In this manner, the relative degree of crystallinity was plotted.

$$X(t) = \frac{\int_0^t \left(\frac{dH}{dt}\right) dt}{\int_0^\infty \left(\frac{dH}{dt}\right) dt} = \frac{A_t}{A_\infty} \quad \textbf{(2)}$$

Where numerator, A_t, is the area under DSC curve from t = 0 to t and denominator, A_∞, is the total area under the crystallization curve.

III. Crystallization behavior by Ozawa equation.

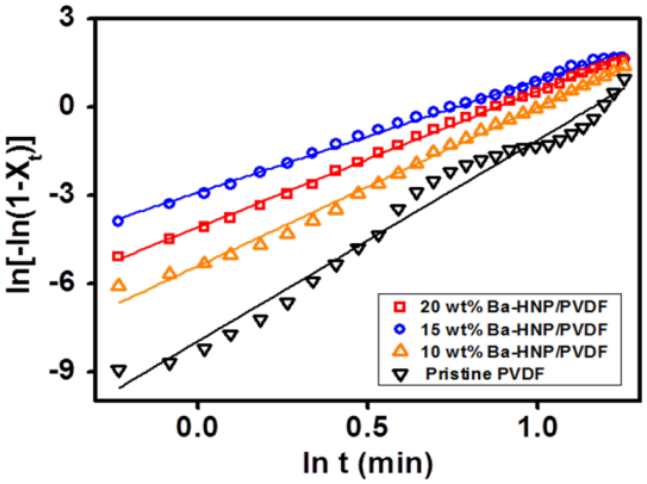

Fig. S3 The plot of $ln[-ln(1-X_t)]$ versus *In t* for thermal behavior parameters.

Natural logarithmic form of Ozawa equation was used to investigate non-isothermal crystallization of kinetics by considering the cooling rate.

$$ln[-ln(1-X_t)] = ln\,k + n\,ln\,t \quad \textbf{(3)}$$

Where X_t the temperature-dependent relative crystallinity, t is the duration of the crystallization, k is the constant of crystallization rate and n is the Ozawa exponent. It indicates a double logarithmic plot of $ln[-ln(1-X_t)]$ verse *ln t* for each sample. Espcially, higist crystallization rate constant (k) of 0.05448 was obtained with 15 wt% and values of Ozawa exponent (n), 2.016 and reaching helf-time crystallinity ($t_{1/2}$), 1.694 μs. The values of the crystallization rate increase with contents of Ba-HNPs until the 15 wt% as expected, but when concentration of filler exceeded 20 wt % caused decreasing value. Moreover, it observed same tendency from crystallization half-time. In other word, it was demonstrated that showing highest crystallization rate of 15 wt% Ba-HNPs/PVDF implies fastest crystallization growth time.

Table. S3 Values of *n*, *k* and $t_{1/2}$ for pristine PVDF and various concentration of Ba-HNPs/PVDF.

Sample	n [a]	k [a]	$t_{1/2}$ (min) [a]
Pristine PVDF	3.004	0.00035	2.301
10 wt% Ba-HNP/PVDF	2.624	0.00447	1.946
15 wt% Ba-HNP/PVDF	2.016	0.05448	1.694
20 wt% Ba-HNP/PVDF	2.572	0.01667	1.813

a These values were obtained by Ozawa analysis of samples using DSC.

5. Observed polarized optical microscopy (POM) of the crystal growth.

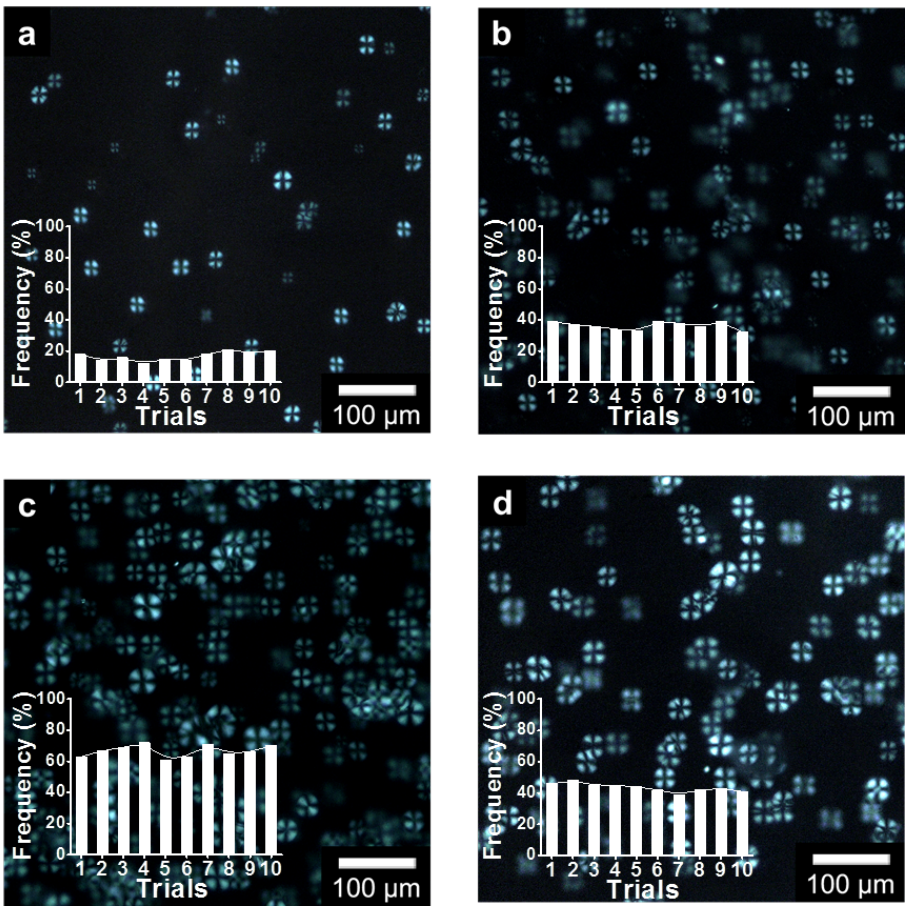

Fig. S4 Polarized optical microscopy image of a) pristine PVDF, b) 10 wt% Ba-HNP/PVDF, c) 15 wt% Ba-HNP/PVDF, and d) 20 wt% Ba-HNP/PVDF. All samples were isothermally crystallized at 160 °C for 240 s and repeated 10 times.

Fig. S4 shows that observed polarized optical microscopy morphology (POM) of the crystal growth. All samples were isothermally crystallized at 170 °C and maintained for 240 s, and it was repeated 10 times to observe crystal growth tendency. After it cooled down, same procedure was repeated 10 times to obtain accurate tendency of crystal growth morphology. The amounts of spherulites were significantly increased by loading concentration of Ba–HNPs. It means that added Ba-HNPs act as nuclei for PVDF crystallization and alter the kinetics of crystallization at constant time. According to the charge-charge interaction of Ba-HNPs and with $-CF_2$ dipole, α crystalline PVDF chains have converted to trans-trans conformation. As a result, reinforced crystallization behavior is intimatly proprotional to content of β phase.

6. Obtained permittivity parameters of Ba-HNPs/PVDF.

Polarizability by addition of Ba-HNPs filler can be estimated by Havriliak-Negami and Fourier transfer relationship,

$$\varepsilon^* = \varepsilon' + i\varepsilon'' = \varepsilon_\infty + \frac{\Delta\varepsilon}{1+(i\omega\lambda)^{1-\alpha}} \quad \textbf{(4)}$$

Where ε' is dielectric constant, ε'' is the dielectric loss factor, therefore, polarizability is defined as,

$$\Delta\varepsilon = \varepsilon_S - \varepsilon_\infty \quad \textbf{(5)}$$

ε_S is ε' as $\lim_{\omega\to 0}\varepsilon^*(\omega)$, and ε_∞ is ε' as $\lim_{\omega\to\infty}\varepsilon^*(\omega)$, calculated in Table S4.

Table S4 Relevant dielectric parameter for Ba-HNPs/PVDF composite with various filler contents.

Sample	ε' [a]	$\Delta\varepsilon$ [a]	λ/[μs] [b]
Pristine PVDF thin film	11	4.9	159
10 wt% Ba-HNP/PVDF	16	5.3	80
15 wt% Ba-HNP/PVDF	21	8.1	62
20 wt% Ba-HNP/PVDF	22	8.8	67

a Values were calculated by Havriliak-Negami and Fourier transforms relationship
b Values were obtained by interfacial polarization response by relaxation time.

7. Illustration of magnified Ba-HNPs.

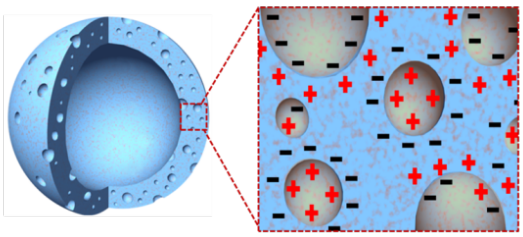

Fig. S5 Schematic representation of the interfacial effect of porous Ba–HNPs. The sketch shows the porous structure of the Ba–HNPs having electrically charged surfaces.

8. THD of acoustic actuator according to nanofiller concentration and various electrodes.

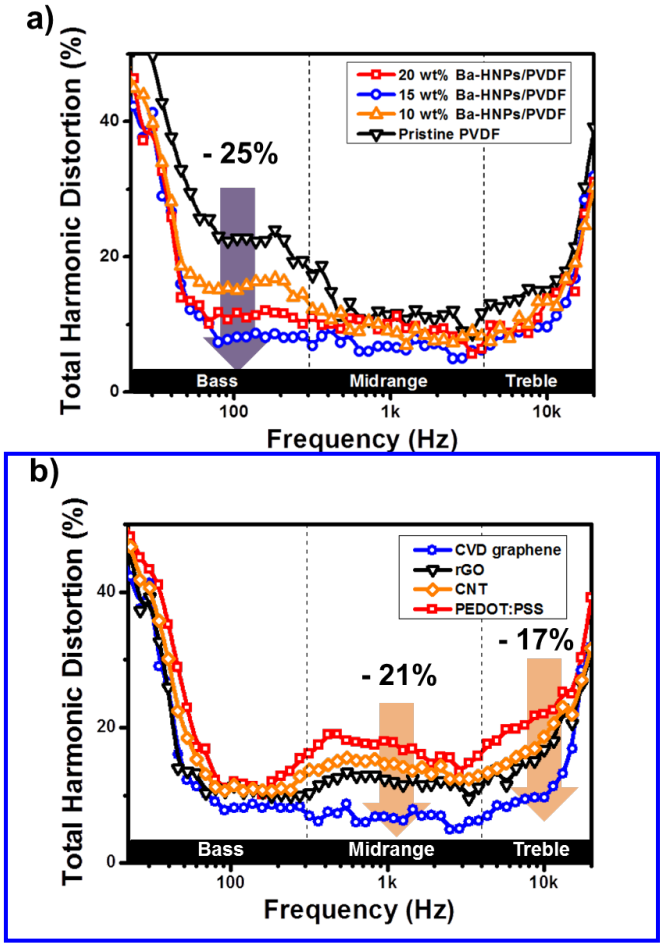

Fig S6 a) THD values of Ba–HNPs/PVDF-based thin film acoustic actuators as a function of Ba–HNPs content. b) THD values for 15 wt% Ba-HNPs/ PVDF film with CVD graphene, rGO, and PEDOT:PSS electrodes. Inkjet printing was used to make the rGO, CNT and PEDOT:PSS-based electrodes having thicknesses of *ca*. 380 nm, 400 nm and 170 nm, respectively. The CVD graphene electrode was wet-transferred onto a silane-treated Ba-HNPs/PVDF film.

Fig. S6a shows the total harmonic distortion (THD) in the bass frequency range with different Ba–HNPs concentration, and the effect of filler content on the frequency response and THD at 100 Hz were sugessted. The behavior of the THD showed simually improved like frequency response and it has decreased by 25 % of THD value with 15 wt% filler content. It showed clear evident that 15 wt% of Ba–HNPs in PVDF was optimum for the thin-film acoustic actuator for maximum sound performance as represented by the frequency response with stable distortion.

9. Transmittance of acoustic actuator with three different electrodes.

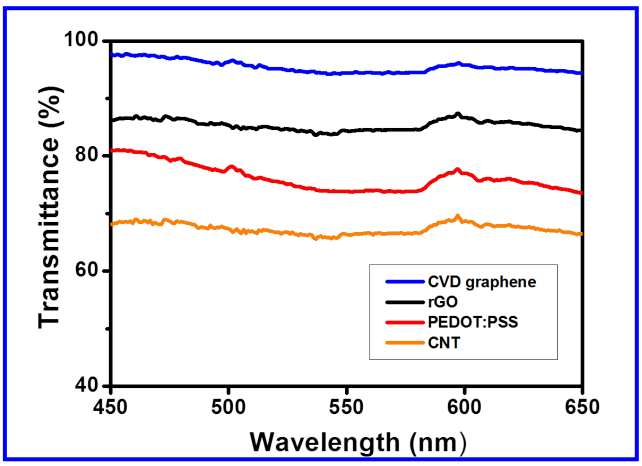

Fig. S7 Transmittance of Ba-HNPs/PVDF-based thin film acoustic actuator with **four** types of electrode.